Syndiotactic polypropylene and its copolymers with alpha-olefins. Effect of composition and length of comonomer

Javier Arranz-Andrés [a], Juan L. Guevara [b,c,d], Teresa Velilla [b,c], Raúl Quijada [b,c], Rosario Benavente [a], Ernesto Pérez [a], María L. Cerrada [a,*]

[a] *Instituto de Ciencia y Tecnología de Polímeros, Juan de la Cierva 3, 28006 Madrid, Spain*
[b] *Departamento de Ingeniería Química, Facultad de Ciencias Físicas y Matemáticas, Universidad de Chile, Casilla 2777, Chile*
[c] *Centro para la Investigación Multidisciplinaria Avanzada en Ciencias de los Materiales (CIMAT), Santiago, Chile*
[d] *Departamento de Química de la Universidad Católica del Norte, Avenida Angamos 0610, Antofagasta, Chile*

Abstract

A set of copolymers of propene and alpha olefins (1-hexene, 1-octene and 1-octadecene) and the corresponding homopolymer (sPP) have been synthesized using a syndiotactic metallocene catalyst. The effect of either the incorporation or length of these conomomeric units on the structure and final properties exhibited has been analyzed. As expected, there is a considerable decrease in crystallinity with the increase of comonomer content. Thus, a completely amorphous copolymer is obtained if the molar fraction is high enough. The structural variations drastically influence the viscoelastic and mechanical behaviors of these copolymers. Three or four relaxation processes can be observed depending on composition and length of comonomer. At temperatures above the process associated with the glass transition (β relaxation), a deep drop (in one or two steps) in E' and a shoulder in E'', overlapped with that β mechanism, are observed. The existence of a relaxation involving crystalline regions is postulated because of its variation with crystal characteristics. Moreover, a relaxation related to internal motions within the comonomeric units is seen in the range of very low temperatures. This process, primarily ascribed to movement of methylenic segments within the comonomer, is strongly depending on composition and length of the pendant aliphatic chains on incorporated units. On the other hand, a decrease in stiffness and microhardness as well as the brittle–ductile transition are observed by simply varying composition when deformation takes place at room temperature.

Keywords: Syndiotactic polypropylene; Comonomer content; Viscoelastic relaxations

1. Introduction

Natta and coworkers synthesized and characterized, around 1960, the syndiotactic form of polypropylene by using vanadium-based catalysts [1]. The stereospecificity reached was not high enough and, therefore, the properties exhibited were poorer than those found in its isotactic counterpart.

Recent progress in metallocene catalysis has led to the development of a wide range of polyolefin materials [2]. The most interesting advancement is that the architecture of the polymer can be tailored by employing a specific catalyst. In the case of the polymerization of propene, it is possible to obtain new microstructures with interesting physical properties, for instance, highly syndiotactic polypropylene and syndiotactic copolymers of propene with other alpha-olefins and higher incorporations.

Isotactic polypropylene, iPP, is highly crystalline with a high strength [3] while syndiotactic polypropylene, sPP, develops a lower degree of crystallinity and, consequently, is more ductile at room temperature with a greater impact strength [4]. In addition, the mechanical and thermal performance of sPPs show a large scatter as a function of stereo and regioregularity of their chains that governs the crystallization. Metallocene catalyzed sPP can be an elastomeric alternative to iPP for some applications, without significant differences in thermal properties required for a particular application. Moreover, sPP might have strong possibilities of being copolymerized with alpha-olefins of different lengths.

The conformation of sPP chains in the crystal was predicted by Natta et al. [5] and confirmed [6] by wide-angle X-ray

* Corresponding author. Tel.: +34 91 5622900; fax: +34 91 5644853.
E-mail address: mlcerrada@ictp.csic.es (M.L. Cerrada).

diffraction (WAXD) and infrared spectroscopy (IR). The preferred conformation is the twofold helical structure with a *ttgg* conformation where *t* is a trans dihedral angle of 180° and *g* a gauche dihedral angle of 60°. This chain conformation might be right or left-handed translated. In the crystal, the ordered packing of these $4\times2/1$ helices leads to an orthorhombic lattice with different unit cells [7–9]. A second conformation is an approximately iso-energetic planar zigzag form with a chain conformation of *tttt* [10,11]. At low temperature, quenched orthorhombic lattice results from packing all-*trans* chains. Finally, under specific circumstances, a monoclinic lattice is developed in which the chain conformation is intermediate between the planar zigzag and the helical forms. In this case, the chains are assumed to be arranged into a $t_6g_2t_2g_2$ conformation [12,13].

The possibility that sPP chains exist in three different conformations (the stable twofold helix, the planar zigzag, and the intermediate $t_6g_2t_2g_2$ conformation) leads to the observed polymorphism, which is highly dependent on crystallization conditions (such as supercooling and crystalization/annealing time) as well as on the chain stereoregularity, molecular weight, and molecular weight distribution. The different crystalline forms are named as follows [8]: two different orthorhombic crystalline forms denoted Form I (ordered and disordered, both with helical conformations); the metastable Form II (orthorhombic with isochiral packing of helical chains according to the space group $C222_1$); the trans planar Form III and the monoclinic Form IV.

Studies on the synthesis and characterization of copolymers of syndiotactic propene with 1-butene, ethylene, 4-methyl-pentene and 1-hexene have recently appeared in the literature [14–24]. Although some work has been also performed in copolymers with 1-octene [25–28], to our knowledge, there are not publications about either the study of properties or synthesis and characterization of syndiotactic propene copolymers with long alpha-olefins. Therefore, the goal of the present work is to examine, for first time, structural details and final properties of several copolymers of propene with 1-hexene, 1-octene and 1-octadecene comonomers, obtained with a syndiospecific catalyst. The effect of composition and length of the pendant alkyl chain on the incorporated alpha-olefinic comonomer is analyzed through the characterization of the thermal properties using differential scanning calorimetry (DSC), of the crystalline structure by either wide or small angle X-ray diffraction, of the viscoelastic behavior by means of dynamic-mechanical thermal analysis (DMTA) and of the mechanical response using uniaxial tensile stress–strain and microhardness measurements.

2. Experimental

Syndiotactic polypropylene and several copolymers of propene with 1-hexene, 1-octene and 1-octadecene olefins (abbreviated CsPH, CsPO and CsPOD, respectively) were synthesized with a syndiospecific catalyst as described elsewhere [29,30]. The homogeneous metallocene syndiospecific catalyst and cocatalyst employed were $Ph_2C(Flu)(Cp)ZrCl_2$ and methylaluminoxane (MAO), respectively. The characteristics of the polymers are reported in Table 1. The composition was determined by the analysis of the ^{13}C NMR solution spectra at 120 °C in deutered tetrachloroethane. The copolymers, according to this analysis, are random and presumably homogeneous in composition.

Films were obtained by compression molding in a Collin press between hot plates (180 and 150 °C for the homopolymer and copolymers respectively) at a pressure of 2 MPa for 4 min, and a subsequent quenching to room temperature between plates refrigerated with water. These films were left at room temperature for several days prior to performing any analysis.

The thermal properties were carried out in a Perkin–Elmer DSC-7 calorimeter connected to a cooling system and calibrated with different standards. The sample weight ranged from 6 to 8 mg. The scanning rate used was 20 °C min^{-1}. For crystallinity determinations, a value of 196.6 J g^{-1} has been taken as the enthalpy of fusion of the perfect crystal of sPP [31]. The glass transition temperature, T_g, was determined as the temperature where the specific heat increment is the half of the total one at the transition.

Wide-angle X-ray diffraction (WAXS) patterns were recorded in the reflection mode at room temperature by using a Philips diffractometer with a Geiger counter, connected to a computer. Ni-filtered Cu K_α radiation was used. The diffraction scans were collected over a period of 20 min in the range of 2θ values from 3 to 43°, using a sampling rate of 1 Hz. The goniometer was calibrated with a silicon standard.

The samples were also studied by small-angle X-ray scattering (SAXS) employing synchrotron radiation (with $\lambda=$ 0.150 nm) in the beamline A2 at HASYLAB (Hamburg,

Table 1
Sample characteristics of the materials analyzed

Sample	Comonomer	Comonomer content		10^{-3} M_w(g mol^{-1})	M_w/M_n
		mol%	wt%		
SPP	–	0.0	0.0	440	2.0
CsPH2.9	1-Hexene	2.9	5.6	358	1.9
CsPH8.0	1-Hexene	8.0	14.8	322	2.0
CsPO3.3	1-Octene	3.3	8.3	218	2.0
CsPO8.1	1-Octene	8.1	19.0	189	1.9
CsPO15.1	1-Octene	15.1	32.2	166	2.1
CsPOD2.2	1-Octadecene	2.2	11.9	388	2.2
CsPOD7.1	1-Octadecene	7.1	31.4	374	1.9

Germany) at room temperature and at a distance of 235 cm from sample to detector. The calibration was performed with the different orders of the long spacing of rat-tail cornea ($L=$ 65 nm). The setup was found to cover a spacings range from 5 to 55 nm.

Viscoelastic properties were measured with a Polymer Laboratories MK II dynamic mechanical thermal analyzer, working in a tensile mode. The temperature dependence of the storage modulus, E', loss modulus, E'', and loss tangent, tan δ, was measured at 1, 3, 10 and 30 Hz over a temperature range from -150 to 120 °C at a heating rate of 1.5 °C min^{-1}. The specimens used were rectangular strips 2.2 mm wide, around 0.7 mm thick and over 15 mm long. The apparent activation energy values were calculated according to an Arrhenius-type equation, employing an accuracy of ± 1 °C in the temperature assignment of E'' maxima. The frequency dependence with temperature in the relaxations associated with the glass transition has also been considered to follow an Arrhenius behavior though it is due to cooperative motions [32]. This approximation can be made without a significant error, since the interval of analyzed frequencies is short enough to be fitted to such a linear behavior as just mentioned.

Stress–strain measurements were performed with an Instron Universal testing machine calibrated according to standard procedures and equipped with a load cell and an integrated digital display that provided force determinations. Dumb-bell shaped specimens with gauge dimensions 15 mm in length, l_0, and 1.9 mm in width were punched out from the sheets with a standardized die. All of the specimens were drawn at a crosshead speed of 10 mm min^{-1} at room temperature. Young's modulus (E), yield stress (σ_y), elongation at break (ε_B) and toughness (T) were determined from the nominal stress–strain measurements. At least four specimens were tested for each material and average values were reported. The error in the mean values was less than 6% except for the elongation at break and toughness estimations, these being higher due to the greater inherent data scattering in the determination of these two magnitudes.

A Vickers indentor attached to a Leitz microhardness tester was used to carry out microindentation measurements. Experiments were undertaken at 23 °C. A contact load of 0.98 N and a contact time of 25 s were employed. Microhardness, MH, values (in MPa) were calculated according to the relationship [33]:

$$\mathrm{MH} = 2\sin 68^\circ P/d^2 \quad (1)$$

where P (in N) is the contact load and d (in mm) is the diagonal length of the projected indentation area.

3. Results and discussion

3.1. Thermal properties

Fig. 1 shows the DSC curves corresponding to the sPP homopolymer. The initial melting (upper curve) presents a clear glass transition at around 5 °C and the main melting endotherm at 117 °C. This rather low melting temperature is due to the relatively low syndiotactic content and causes the sample to have a tail at the low temperature side of the melting curve that extends down to room temperature. Additionally, the appearance of a small endotherm is observed at 50 °C (see upper curve of Fig. 1). This feature might arise from the annealing process related to keeping of the sample at room temperature, as occurs in other olefinic materials [34–36] where the annealing peak appears at a temperature around 15–20° higher than the annealing temperature (room temperature in most cases). Alternatively, considering the complicated polymorphic behavior of sPP aforementioned, this endotherm could be also associated with a transformation (or simply melting) from a polymorph different than the major crystalline structure that melts at 117 °C. This second possibility seems to be unlikely from some preliminary real-time variable temperature WAXS experiments, since the same diffractions are observed in the specimen along the entire temperature interval up to the melting process. However, some additional measurements will be performed to complete this study.

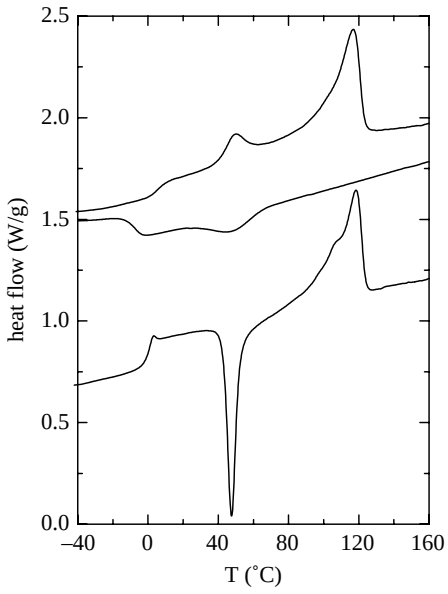

Fig. 1. DSC curves of the sPP homopolymer sample. From top to bottom: first heating, cooling and second heating processes, respectively. Scanning rate: 20 °C min^{-1}.

A total enthalpy of melting of 44 J g^{-1} is deduced from the melting curve, that corresponds to a crystallinity degree of around 22%, this value being also rather low because of the moderately low syndiotactic content.

The middle curve in Fig. 1 represents the cooling of the sPP sample from the melt. It shows a crystallization exotherm, centered at 48 °C, with an enthalpy of only 7 J g^{-1}. Therefore, a minor amount of the sample is exclusively able to crystallize at this cooling rate, 20 °C min^{-1}, owing to the slow crystallization rate exhibited by sPP, contrarily to that observed in its stereoisomer iPP. This characteristic is due to the alternation of methyl groups that confers on sPP a more flexible backbone and leads to a higher density of molecular entanglements

within the molten state [37]. Just after crystallization takes places, the glass transition is observed at around −10 °C.

The subsequent melting (lower curve of Fig. 1) first shows the glass transition, at around 0 °C. A shift to lower temperatures and an appreciably higher specific heat increment are observed compared to that shown during the first melting, due to the lower crystallinity degree developed by the specimen while cooling. At higher temperature, a sharp exotherm, centered at 48 °C and involving around 22 J g^{-1}, is clearly seen. This exotherm represents a cold crystallization of sPP macromolecular segments that were not able to crystallize during cooling at 20 °C min^{-1}. Finally, a main melting endotherm, with a maximum at 118 °C, is observed.

The DSC curves corresponding to the initial melting of the different copolymers are shown in Fig. 2 and compared with that exhibited for the homopolymer. A similar behavior is observed for the tree types of comonomers: the copolymers with lower comonomer content show both the main melting endotherm, at around 80–90 °C, and the 'annealing' one, with a maximum at 49–52 °C. In copolymers with a comonomer content about of 7–8 mol% only one endotherm is observed located at temperatures close to the annealing peak. The comonomer molar fraction in these copolymers is high enough to lead to the development of crystallites with a small size, melting within this temperature interval. Finally, copolymer CsPO15.1 shows only the glass transition, i.e. this sample is completely amorphous since the content of 1-octadecene breaks down the regularity of chains and, consequently, its capability of tridimensional organization (at least under the current thermal history).

The values of the different peak temperatures and crystallinity deduced from those melting curves are presented in Table 2. As expected, the melting temperature and the crystallinity are very much dependent on the comonomer content, the former magnitude shifting to lower temperatures and the second one diminishing as incorporation of comonomer increases in the distinct families of copolymers. To compare the effect of the comonomer length on the thermal behavior, the degree of crystallinity has been normalized to the sPP weight content in the copolymer (see Table 2) since these types of alpha-olefinic branches cannot be incorporated into the crystalline structure [38–40]. It can be deduced that crystallinity in the 1-hexene copolymers decreases linearly to a lesser extent than the other two copolymers that also decrease in crystallinity with increasing comonomer composition.

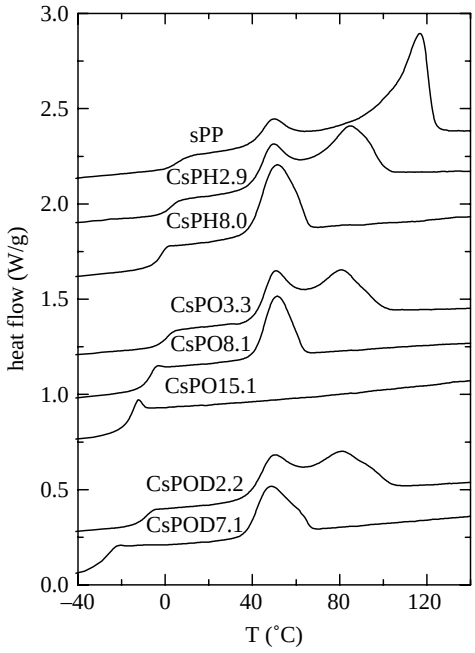

Fig. 2. DSC first melting curves of the homopolymer and copolymers. From top to bottom: sPP, CsPH2.9, CsPH8.0, CsPO3.3, CsPO8.1, CsPO15.1, CsPOD2.2 and CsPOD7.1. Heating rate: 20 °C min^{-1}.

Another interesting feature from the DSC heating curves is the behavior of the glass transition. A significant variation of T_g is observed with both the comonomer content and the type of comonomer, as depicted in Figs. 2 and 3 for the initial melting. It seems clear that the depression of the glass transition is deeper as either composition or length of comonomer increase in the copolymer. Thus, a reduction of around 31 °C is observed in the case of the copolymer CsPOD7.1, although it has to be considered that this sample incorporates a 31.4% by weight of 1-octadecene comonomer.

Regarding the cooling process of these copolymers, none of them exhibits any appreciable crystallization exotherm at the regular cooling rates in the calorimeter. Moreover, the subsequent melting curves do not display a cold crystallization for any of the copolymer samples, as seen in Fig. 4, and only the glass transition is observed. Therefore, the copolymers are completely amorphous because they cannot be crystallized in the empirical time scale since their crystallization rate is even slower than that presented by sPP homopolymer, which shows a crystallization process during this second heating additionally to a melting endotherm. The corresponding values of the glass transition temperature for this second melting are listed in the last column of Table 2. These are rather similar to those found along the initial melting, especially for the higher comonomer contents, due to their low capability for crystallizing even after a stay at room temperature. However, in the homopolymer and copolymers with low contents, independently of the type of comonomer, the differences in glass transition temperatures are significant: T_g in the first melting being at about 5° higher, due to the constraints within the amorphous regions imposed by the 'considerable' amount of crystallinity developed during the maintenance of these samples at room temperature.

The motion restrictions caused by crystallites also affect the facility of enthalpic relaxation [41] within amorphous regions below their glass transition. The small endotherm located at the top of the glass transition reflects the magnitude of this process when a sample stays below T_g during the cooling and heating cycles. In Figs. 1, 2 and 4, it can be clearly observed that the small endotherm is inversely related to the crystallinity of the sample. During the first heating, this process is almost absent in those specimens with a 'considerable' crystallinity whereas it is well-evident in the second melting curves for the copolymers, since they are completely amorphous.

Table 2
DSC values of the glass transition and melting temperatures (first melting), DSC and X-ray crystallinities, crystal size determined by SAXS measurements and glass transition temperature in the second melting

Sample	T_g (°C)	T_m (°C)	$f_c^{DSC\ NORM}$	$f_c^{RX\ NORM}$	I_c (nm)	T_g^{F2} (°C)
SPP	5	117	0.22	0.27	2.7	0
CsPH2.9	2	85	0.19	0.23	2.3	−3
CsPH8.0	−2	51	0.12	0.14	1.4	−5
CsPO3.3	0	81	0.16	0.17	1.7	−5
CsPO8.1	−8	52	0.09	0.09	0.9	−9
CsPO15.1	−17	–	0.00	0.00	–	−17
CsPOD2.2	−10	81	0.18	0.18	1.8	−11
CsPOD7.1	−26	49	0.10	0.10	1.0	−26

The values of crystallinities have been normalized to the corresponding sPP weight content in the different samples.

3.2. Structural characterization

The X-ray diffractograms of the different samples, acquired at room temperature, are shown in Fig. 5. It is evident that even the homopolymer exhibits a rather low crystallinity. It develops the disordered Form I that consists of an orthorhombic lattice where disorder comes from the alteration of right- and left-handed helices along both axes of the unit cell [9]. In addition, for specimens isothermally crystallized below 120 °C, this disorder can be also arisen from defects in the stacking of the *bc* layers of chains along a, implying *b*/4 shifts among consecutive layers. Four diffractions are characteristic of the crystalline lattice in the 2θ representation at around 12.2, 15.8, 20.8 and 24.5°, corresponding to the (200), (010), (111) and (400) reflections, respectively [7–9].

The incorporation of a comonomer leads to a broadening of the diffraction peaks and a decrease in their intensity, both characteristics associated with crystallites of smaller size (as measured in SAXS experiments—see Table 2) and/or crystallite perfection, and with a reduction of the crystallinity. These features become more significant as comonomer content increases due to the difficulty of incorporating the long alkyl chains of the comonomer into the crystal lattice.

The bottom diffractogram in Fig. 5 presents a completely amorphous pattern that corresponds to an efficiently quenched and rapidly analyzed sPP sample, which possesses a lower stereospecificity than that exhibited by the sPP under study (the fully syndiotactic pentads are 63 and 80%, respectively). Therefore, it has been taken as amorphous profile of sPP. It is worth noting that preparation of amorphous sPP is not simple and the quenching at 0 °C induces formation of its mesomorphic form [42–50] for specimens with relatively high syndiotacticity. It has to be said that it is practically identical to that found for an elastomeric totally amorphous polypropylene sample [51]. This sPP amorphous halo has been utilized for the determination of the degree of crystallinity developed in the homopolymer and the copolymers with low comonomer content, similar to what we previously did for isotactic polypropylenes [52,53], their blends [54,55] and their copolymers with alpha-olefins [56]. However, a certain

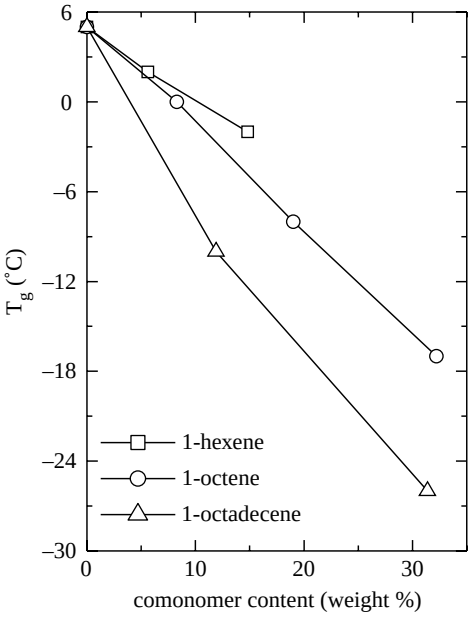

Fig. 3. Dependence of glass transition temperature with weight comonomer content, for the different types of copolymers.

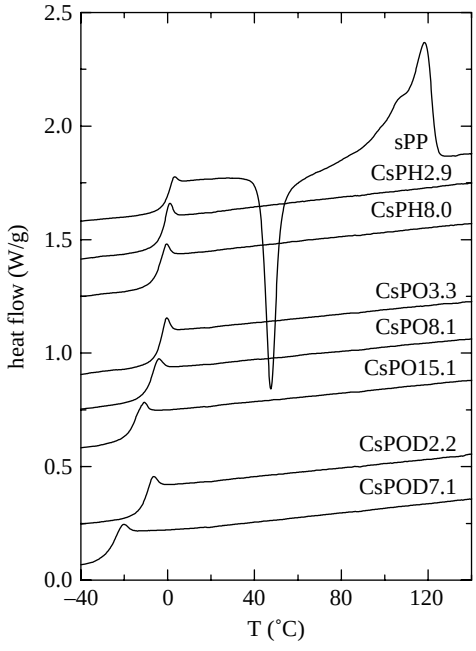

Fig. 4. DSC second melting curves in the homopolymer and copolymers. From top to bottom: sPP, CsPH2.9, CsPH8.0, CsPO3.3, CsPO8.1, CsPO15.1, CsPOD2.2 and CsPOD7.1. Heating rate: 20 °C min^{-1}.

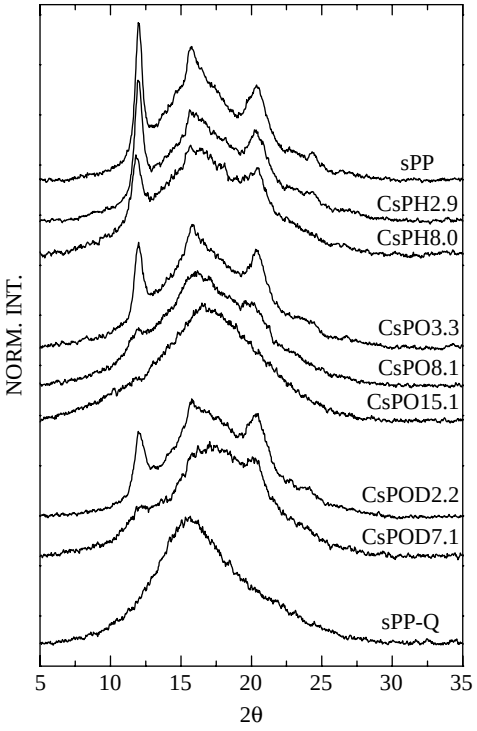

Fig. 5. X-ray diffraction patterns, at room temperature, of the different samples. From top to bottom: sPP, CsPH2.9, CsPH8.0, CsPO3.3, CsPO8.1, CsPO15.1, CsPOD2.2, CsPOD7.1 and sPP-Q (an efficiently quenched sPP sample with the fully syndiotactic pentads of 63%).

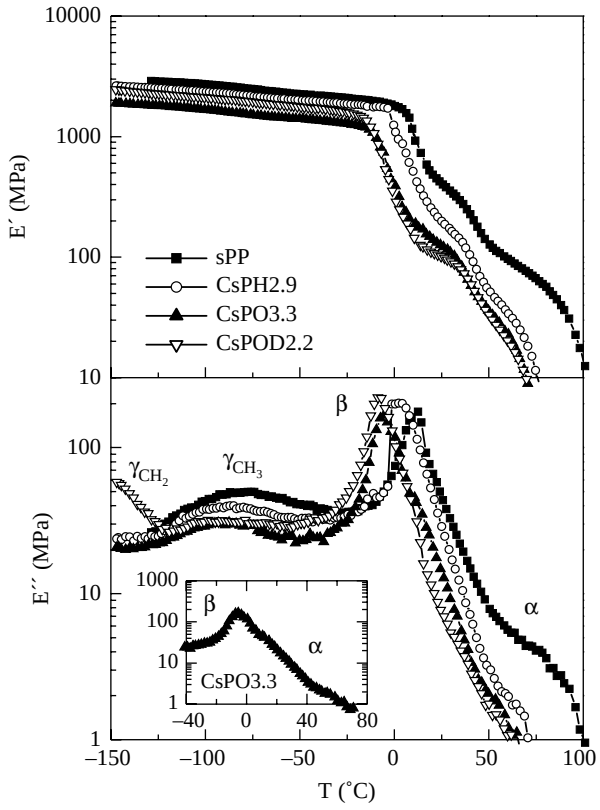

Fig. 6. Temperature dependence of the real and imaginary components of complex modulus for sPP, CsPH2.9, CsPO3.3 and CsPOD2.2.

additional contribution at 2θ around 17–18° has been considered in the copolymers with intermediate and high comonomer compositions to obtain the corresponding pure crystalline profiles. This contribution may arise in these copolymers under study from the coexistence of a certain amount of disordered modification of Form II containing kink-bands together with Form I similarly to results found in copolymers with ethylene and 1-hexene isothermally crystallized [17].

The values of the degree of crystallinity obtained by WAXS are reported in Table 2. If they are compared with those determined from DSC measurements, slightly higher values are achieved from X-ray diffractograms, although both determinations provide rather similar results for the copolymers with high comonomer contents. It has to be indicated that the degree of crystallinities listed in Table 2 have been normalized taking into account the weight percentage of sPP in the sample since it is assumed that the three comonomers are long enough to be totally excluded from the sPP crystal lattice. This normalization is really important when the comonomer content is rather high or when the length of the comonomer pendant chain is very long: for instance, almost one third of the sample weight is not sPP for CsPO15.1 and CsPOD7.1 copolymers.

3.3. Dynamic-mechanical properties

Figs. 6 and 7 show plots of storage and loss moduli, and tan δ as a function of temperature for the homopolymer and some copolymer specimens. There is a controversy in the literature concerned to the number of relaxation processes existing in sPP. Therefore, the different relaxations observed either in sPP or in its copolymers are analyzed separately in order of decreasing temperatures as follows.

3.3.1. The α-relaxation

There remains no clear consensus regarding the origin, and even the existence, of this process, that occurs at temperature above that relaxation related to the glass transition (β mechanism). There is a body of opinions which supports the absence [57,58] of any relaxation above the β process for sPP. However, its presence is recognized by some other authors [59,60] though its origin it is not clear. On the one hand, a second glass transition has been proposed [59] similar to what has been described by some researchers [61,62] in its stereoisomer iPP. On the other hand, this α relaxation has been related to a change in the modes of force transmission or, more precisely, a change in the mechanical coupling of the force-transmitting rigid crystalline entities [60].

The results found in the present investigation show two clear drops in E' above that associated with the glass transition of the homopolymer sPP and the copolymers with the lowest comonomer content, CsPH2.9, CsPO3.3 and CsPOD2.2. The reduction of rigidity around the glass transition (β process) in sPP is significantly less than that observed for the copolymers depicted in Fig. 6 due to the high mobility restrictions within the amorphous phase in sPP (arising from higher crystallinity

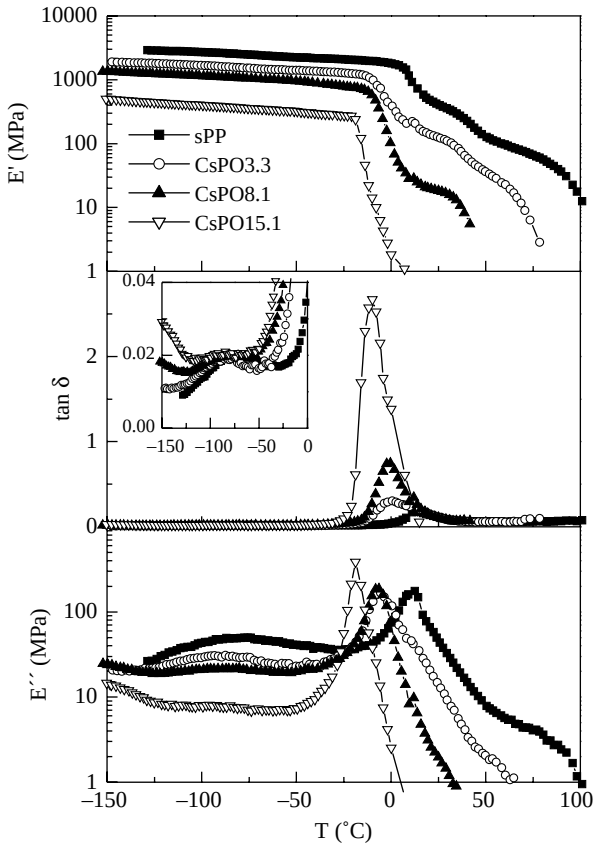

Fig. 7. Temperature dependence of the real and imaginary components of complex modulus and loss tangent of sPP homopolymer and its copolymers with 1-octene.

and larger crystallites). Therefore, these two losses of stiffness at high temperatures are less pronounced in these copolymers than in sPP since both rigidity drops appear more superimposed in the copolymers. Looking carefully at the E'' representation of Fig. 6 and its insert, it is observed that the β relaxation is asymmetric in the side of highest temperatures, pointing out the overlapping of this cooperative movement with another more local motion. However, an unambiguous peak is not observed in tan δ plots, as depicted in Fig. 7. We think that a relaxation process related to motion that involves crystalline regions, in some extent, is taking place, as occurred in iPP [32,63]. The lower crystallinity developed in sPP coupled with the smaller size of their crystallites, compared to those obtained in iPP, may make these crystalline entities more mobile at lower temperatures and over a narrower temperature range. Though a unique global process is considered, two E' drops are observed: the first one above the β process might be associated with the melting of the smaller crystallites and the motions of those that are slightly larger. Since the enthalpy associated with this melting process is significant, the loss of rigidity is also important. The second decrease would be related to motion of larger crystallites.

3.3.2. The β-relaxation

This process is identified with the glass transition of sPP and the different copolymers. Therefore, this relaxation is related to generalized motions in the amorphous regions and its intensity and location are strongly dependent on content and type of comonomer in the copolymer. As comonomer content increases, the amorphous regions exhibit a higher mobility, due to the reduction in the number and size of crystallites and, additionally, the amount of the material that contributes to this cooperative mechanism is higher. Consequently, it occurs at lower temperature and its intensity is increased, as depicted in Fig. 7.

On the other hand, for a similar comonomer content it seems that the copolymers with 1-octadecene exhibit this process associated with cooperative motions at lower temperatures (see Table 3), as also observed in the values of T_g determined by DSC. It might be due to the existence of a higher free volume fraction because of their longer lateral branches.

Table 3
Relaxation temperatures (E'' basis at 3 Hz) and apparent activation energies for two of the different viscoelastic processes in sPP and copolymers

Sample	T (°C)		ΔH (kJ mol^{-1})	
	$T_\gamma^{CH_3}$	T_β	$\Delta H_\gamma^{CH_3}$	ΔH_β
sPP	−78	11	55	>400
CsPH2.9	−87	3	55	335
CsPH8.0	−86	2	50	370
CsPO3.3	−90	−5	70	380
CsPO8.1	−88	−7	40	355
CsPO15.1	−103	−18	30	>400
CsPOD2.2	−90	−8	35	365
CsPOD7.1	−90	−24	–	290

3.3.3. The γ^{CH_3}-relaxation

This process is observed at around −80 °C. It is attributed to local motions of methyl groups directly connected to main backbone in sPP and copolymers. This relaxation is quite less broad than that with similar molecular origin found in iPP [32, 63] because of the lower steric restrictions between the alternant methyl groups. As the conomomer content increases, its intensity is lowered due to the lower content of methyl groups, and its location is shifted to lower temperatures probably due to the ease of this rotational motion. For a similar comonomer content, a decrease in intensity and a narrowness of the relaxation time distribution are observed. These two features might be related to a major free volume fraction with length of comonomer.

3.3.4. The γ^{CH_2}-relaxation

Moreover, an additional γ^{CH_2} process is seen at around −150 °C in the copolymers with the highest content of either 1-hexene or 1-octene and in the two 1-octadecene copolymers. The molecular cause of this relaxation is different from that of the γ^{CH_3} process of polypropylene. It seems that it is directly related to the comonomer incorporation, as deduced from Fig. 8 for this temperature range in the tan δ plot. This feature seems to point out that this relaxation might be associated with the joint movements of chains containing three or more methylene units, i.e. its inherent origin should be analogous to that responsible for the typical γ relaxation observed in

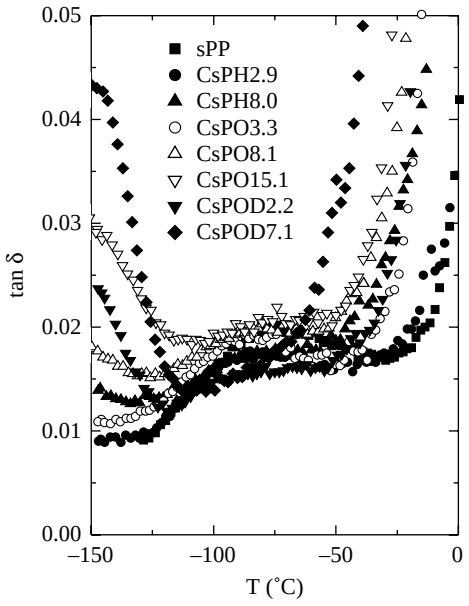

Fig. 8. Loss tangent values at low temperatures for the different specimens analyzed.

polyethylene. Therefore, as comonomer content increases there is a higher amount of methylene groups that can undergo this motion and it is detected by this technique. Consequently, it is not very obvious for the copolymer CsPH8.0 whereas it is completely evident for CsPO15.1 and appears visibly in both copolymers with 1-octadecene, even in that with a low molar fraction (CsPOD2.2).

3.4. Mechanical response

3.4.1. Stress–strain measurements

Fig. 9 shows the stress–strain behavior of the homopolymer and the different copolymers synthesized. The homopolymer shows the typical deformation regions of a classic semicrystalline polymer: an elastic zone followed by a marked yielding point (transition from elastic to plastic deformation, reversible and irreversible respectively), cold-drawing and, finally, the strain hardening.

This figure also displays the great effect of the incorporation of the comonomer in the stress–strain behavior and in the subsequent parameters obtained for the different materials. In particular, Fig. 9 depicts an important change in the homopolymer and the lowest content copolymers that occurs at the yielding region where the cross sectional area starts to decrease more rapidly at one particular point along the gauge length as a neck starts to form. The nominal stress falls significantly after the yield and settles at a constant value as the neck extends along the specimens. The difference between the stress at yielding point and that reached during the necking propagation diminishes with the amount of comonomeric units incorporated and a change from cold-drawing to homogeneous deformation is observed. It seems that as the length of the comonomer is increased a lower content of that comonomer is needed to change the deformation mechanism. Therefore, in

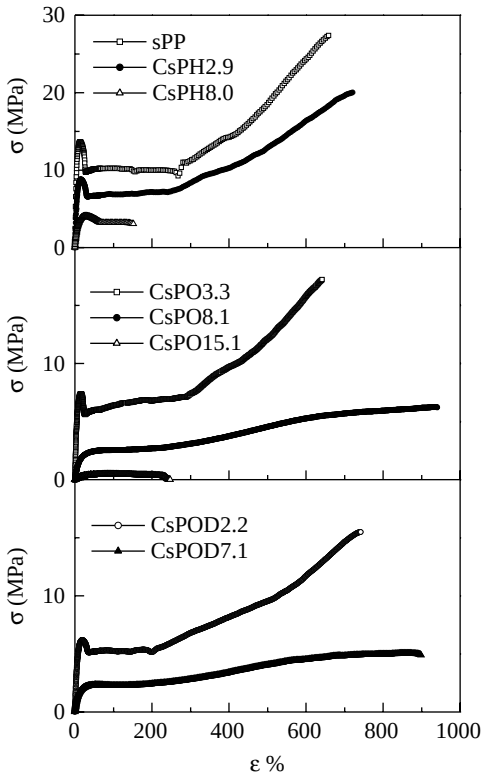

Fig. 9. Stress–strain curves for the sPP and its alpha-olefinic copolymers, at room temperature and 10 mm min^{-1}.

the copolymers with 1-hexene the deformation takes place through a necking formation even in CsPPH8.0. These variations can be ascribed to the structural details within the distinct specimens, such as the percentage of crystallinity and crystallite size [64] coupled with a feasible plasticizer effect of the branches. Therefore, a reduction of rigidity (and so elastic modulus) and yielding stress together with an increase in the yielding strain, are attained as comonomer content increases in the copolymer (see Fig. 10).

A significant recovery phenomenon is observed after rupture of specimens because of the high elasticity of sPP and its copolymers. The percentage of this is listed in Table 4.

Toughness is another important mechanical property, that can be defined in several ways, one of which is in terms of the area under the stress–strain curve [65]. Toughness is, therefore, an indication of the energy that a material can absorb before breaking. The sPP and its alpha olefinic copolymers are tough because of their inherent elasticity, their low values of crystallinity and their small crystallites. It can be observed that specimens that stretch through neck formation are tougher than those that deform homogenously. Therefore, the final strain hardening process in the former mechanism seems to be more effective in increasing toughness than the viscous flow of chains responsible for the quasi-homogeneous deformation observed as comonomer content increases. The orientation induced within macromolecules during hardening considerably increases the stress values throughout the strain whereas reorientations of chains and/or their simply sliding occurring in

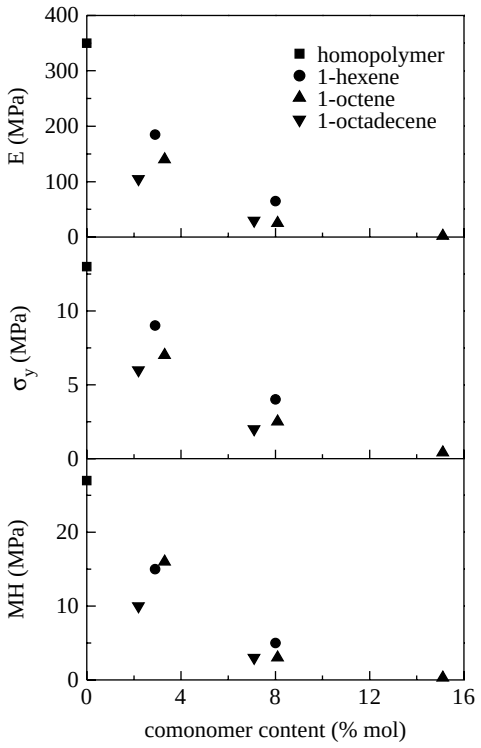

Fig. 10. Variation of Young's modulus (E), yield stress (σ_Y) and microhardness (MH) as a function of comonomer content.

the homogenously deformed copolymers do not lead to such an stress increase.

3.4.2. Microhardness measurements

The hardness of a material can be defined as a measurement of the resistance to a permanent deformation or damage. The deformation of a polymer under the action of the indenter is basically ruled by the viscoelastic and plastic components that also govern the mechanical properties of the material. Microhardness involves a complex combination of properties (elastic modulus, yield strength, strain hardening, toughness). Therefore, it can also be expected that microhardness is related to structural parameters since mechanical properties are structure-dependent. These relationships allow microhardness measurements to be used as a non-destructive testing technique [66]. Fig. 10 shows that the effect of the comonomer content on the MH is similar to that found in the elastic modulus, confirming its relationship with stiffness. Thus, a decrease in MH values is observed when the comonomer content increases. An empirical equation [33] was proposed to indicate the correlation between these two mechanical parameters, expressed by:

$$MH = aE^b$$

where a and b are constants. A quite good linear fit ($R^2 = 0.991$) is obtained in the double-logarithmic scale, as shown in Fig. 11, confirming the validity of this equation for this set of copolymers. This figure represents both the elasticity modulus from tensile deformation and the storage modulus obtained by DMTA measurements, since they characterize the same physical magnitude.

4. Conclusions

The sPP homopolymer sample studied here shows a very low crystallization rate that is even much lower in the case of its copolymers with different alpha-olefin comonomeric units. Thus, a cold crystallization is observed during the sPP heating just after its cooling from the molten state whereas its copolymers are completely amorphous just after cooling.

All of the specimens develop the disordered Form I during their stay at room temperature for several days (except CsPO15.1 that is completely amorphous because of its very high comonomer content). The incorporation of comonomer leads to a broadening of the diffractions and a decrease in their intensity, both characteristics associated with crystallites of smaller size and a lower value of crystallinity, confirming the results obtained by DSC. In these copolymers is probable the coexistence of disordered Form I with disordered modification of Form II.

Three or four relaxation processes can be observed depending on composition and length of comonomer. At temperatures above the process associated with the glass transition (β relaxation), a deep drop (in one or two steps) in E' and a shoulder in E'', overlapped with that β mechanism, are observed and its relationship with a relaxation involving the crystalline regions is postulated because of its variation with crystal characteristics. Moreover, a relaxation related to internal motions within the comonomeric units (labeled as γ^{CH_2}) is seen in the range of very low temperatures. This

Table 4
Mechanical parameters of the different samples, analyzed at 23 °C and stretched at 10 mm min^{-1}

Sample	E (Mpa)	σ_Y (MPa)	ε_Y (%)	σ_B (MPa)	ε_B (%)	R (%)	T (kJ m^{-2})	MH (MPa)
sPP	350	13	13	22	575	68	1130	27
CsPH2.9	185	9	16	17	645	84	965	15
CsPH8.0	65	4	28	3	135	–	75	5
CsPO3.3	140	7	16	16	610	91	814	16
CsPO8.1	25	2.5	14	6	785	93	466	3
CsPO15.1	2	0.4	30	0.4	180	86	130	0.3
CsPOD2.2	105	6	19	14	715	85	860	10
CsPOD7.1	30	2	65	5	845	89	460	3

Young's modulus, E; yield stress, σ_Y; yield deformation, ε_Y; stress at break, σ_B; deformation at break, ε_B; recovery percentage, R; toughness, T, and microhardness, MH.

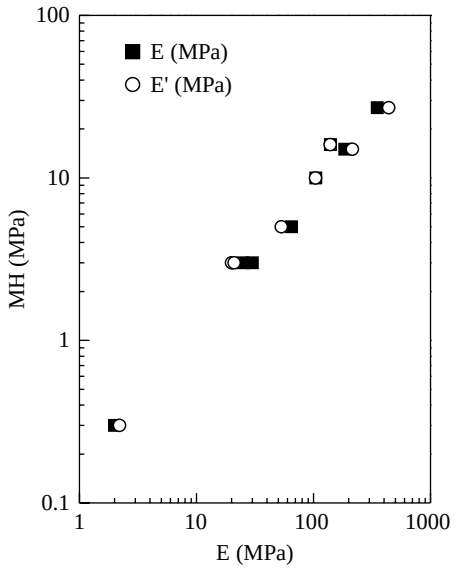

Fig. 11. Relationship between microhardness, MH, and elastic moduli (E and E') for the different samples.

process, primarily ascribed to movements of methylenic segments within the comonomer, is strongly dependent on composition and length of incorporated units.

On the other hand, a decrease in stiffness and microhardness as well as the brittle–ductile transition are observed by simply varying composition, when deformation takes place at room temperature. Moreover, a significant recovery phenomenon is attained just after rupture of specimens because of the high elasticity of sPP and its copolymers. Finally, the strain hardening process, observed in sPP and copolymers that stretch through neck formation, seems to be more effective in increasing toughness than the slippage of chains responsible for the quasi-homogeneous deformation at high strains found as comonomer content increases.

Acknowledgements

The authors are grateful for the financial support of Comunidad Autónoma de Madrid, Ministerio de Educación y Ciencia, CONICYT and the Exchange Collaboration Program CONICYT/CSIC (projects 07N/0093/2002, MAT2004-01547, FONDAP 11980002 and 2003CL0028, respectively). The support from the European Commission (COST Action D17, WG D17/0004/00) is also acknowledged. The synchrotron work (in the A2 polymer line of Hasylab at DESY, Hamburg) was supported by the European Community—Research Infrastructure Action under the FP6 'Structuring the European Research Area' Programme (through the Integrated Infrastructure Initiative 'Integrating Activity on Synchrotron and Free Electron Laser Science'.)(Contract RII3-CT-2004-506008). We thank the collaboration of the Hasylab personnel, specially Dr S. Funari. We are grateful to M. C. Martínez from Repsol YPF for the help in the NMR measurements. J. Arranz-Andrés is also grateful to Ministerio de Ciencia y Tecnología and to Repsol-YPF for the financial support.

References

[1] Natta G, Pasquon I, Zambelli A. J Am Chem Soc 1962;84:1488.
[2] Coates GW. Chem Rev 2000;100:1223.
[3] Gupta VK. In: Cheremisinoff NP, editor. Handbook of engineering polymeric materials. New York: Marcel Dekker Inc.; 1997. p. 115.
[4] Sinclair KB. Proceedings of the international conference on polyolefins VIII. Houston: Society of Plastic Engineering; 1993.
[5] Natta G, Corradini P, Ganis P. Makromol Chem 1960;39:238.
[6] Natta G, Corradini P, Ganis P. J Polym Sci 1962;58:1191.
[7] De Rosa C, Corradini P. Macromolecules 1993;26:5711.
[8] De Rosa C, Auriemma F, Corradini P. Macromolecules 1996;29:7452.
[9] De Rosa C, Auriemma F, Vinti V. Macromolecules 1997;30:4137.
[10] Natta G, Peraldo M, Allegra G. Makromol Chem 1964;75:215.
[11] Chatani Y, Maruyama H, Noguchi K, Asanuma T, Shiomura T. J Polym Sci, Part C 1990;28:393.
[12] Chatani Y, Maruyama H, Asanuma T, Shiomura T. J Polym Sci, Polym Phys 1991;29:1649.
[13] Auriemma F, De Rosa C, Ruiz de Ballesteros O, Vinti V, Corradini P. J Polym Sci, Polym Phys 1998;36:395.
[14] Kakugo M. Macromol Symp 1995;89:545.
[15] Naga N, Mizunuma K, Sadatoshi H, Kakugo M. Macromolecules 1997; 30:2197.
[16] De Rosa C, Talarico G, Caporaso L, Auriemma F, Galimberti M, Fusco O. Macromolecules 1998;31:9109.
[17] Naga N, Mizunuma K, Sadatoshi H, Kakugo M. Polymer 2000;41:203.
[18] De Rosa C, Auriemma F, Orlando I, Talarico G, Caporaso L. Macromolecules 2001;34:1663.
[19] De Rosa C, Auriemma F, Fanelli E, Talarico G, Capitani D. Macromolecules 2003;36:1850.
[20] De Rosa C, Auriemma F, Capitani D, Caporaso L, Talarico G. Polymer 2000;41:2141.
[21] Zhang B, Yang D, De Rosa C, Yan S. Macromolecules 2002;35:4646.
[22] De Rosa C, Auriemma F, Vinti V, Grassi A, Galimberti M. Polymer 1998; 39:6219.
[23] De Rosa C, Auriemma F, Talarico G, Busico V, Caporaso L, Capitani D. Macromolecules 2002;35:1314.
[24] De Rosa C, Auriemma F. Adv Mater 2005;17:1503.
[25] Jungling S, Mulhaupt R, Fischer D, Langhauser F. Angew Makromol Chem 1995;229:93.
[26] Thomann R, Kressler J, Mülhaupt R. Polymer 1998;39:1907.
[27] Thomann R, Kressler J, Mülhaupt R. Macromol Chem Phys 1997;198: 1271.
[28] Hauser G, Schmidtke J, Strobl G. Macromolecules 1998;31:6250.
[29] Guevara JL. PhD Thesis. University of Chile; 2004.
[30] Quijada R, Guevara JL, Galland GB, Rabagliati FM, López-Majada JM. Polymer 2005;46:1567.
[31] Haftka S, Könnecke K. J Macromol Sci Phys 1991;B30:319.
[32] McCrum NG, Read BE, Williams G. Anelastic and dielectric effects in solid polymers. New York: Dover; 1991.
[33] Baltá Calleja F. J Adv Polym Sci 1985;66:117.
[34] Alizadeh A, Richardson L, Xu J, McCartney S, Marand H, Cheung YW, et al. Macromolecules 1999;32:6221.
[35] Cerrada ML, Benavente R, Pérez E. J Mater Res 2001;16:1103.
[36] Cerrada ML, Benavente R, Pérez E. Macromol Chem Phys 2002;203:718.
[37] Wheat WR. SPE ANTEC' conference proceedings 1997 [p. 1968].
[38] Pérez E, VanderHart DL. J Polym Sci, Polym Phys 1987;25:1637.
[39] Pérez E, VanderHart DL, Crist Jr B, Howard PR. Macromolecules 1987; 21:78.
[40] Alamo RG, Viers BD, Mandelkern L. Macromolecules 1993;26:5740.
[41] Struik LCE. Physical aging in amorphous polymers and other materials. Amsterdam: Elsevier; 1978.
[42] Vittoria V, Guadagno L, Comotti A, Simonutti R, Auriemma F, De Rosa C. Macromolecules 2000;33:6200.
[43] Nakaoki T, Ohira Y, Hayashi H, Horii F. Macromolecules 1998;31:2705.
[44] Ohira Y, Horii F, Nakaoki T. Macromolecules 2000;33:1801.

[45] Nakaoki T, Yamanaka T, Ohira Y, Horii F. Macromolecules 2000;33: 2718.
[46] Ohira Y, Horii F, Nakaoki T. Macromolecules 2000;33:5566.
[47] Ohira Y, Horii F, Nakaoki T. Macromolecules 2001;34:1655.
[48] Nakaoki T, Ohira Y, Horii F. Polymer 2001;42:4555.
[49] De Rosa C, Auriemma F, Ruiz de Ballesteros O. Polymer 2001;42:9729.
[50] De Rosa C, Ruiz de Ballesteros O, Santoro M, Auriemma F. Polymer 2003;44:6267.
[51] Mansel S, Pérez E, Benavente R, Pereña JM, Bello A, Röll W, et al. Macromol Chem Phys 1999;200:1292.
[52] Prieto O, Pereña JM, Benavente R, Cerrada ML, Pérez E. Macromol Chem Phys 2002;203:1844.
[53] Arranz-Andrés J, Benavente R, Pérez E, Cerrada ML. Polym J 2003;35:766.
[54] Arranz-Andrés J, Benavente R, Peña B, Pérez E, Cerrada ML. J Polym Sci, Polym Phys 2002;40:1869.
[55] Prieto O, Pereña JM, Benavente R, Pérez E, Cerrada ML. J Polym Sci, Polym Phys 2003;41:1878.
[56] Palza H, López-Majada JM, Quijada R, Benavente R, Pérez E, Cerrada ML. Macromal chem Phys 2005;206:1221–1230.
[57] Sakata Y, Unwin AP, Ward IM. J Mater Sci 1995;30:5841.
[58] Schwarz I, Stranz M, Bonnet M, Petermann J. Colloid Polym Sci 2001; 279:506.
[59] Guadagno L, D'Arienzo L, Vittoria V. J Macromol Sci-Phys 2000;B39: 425.
[60] Men Y, Strobl G. Polymer 2002;43:2761.
[61] Boyer RF. J Macromol Sci- Phys 1973;B8:503.
[62] Wunderlich B, Grebowicz J. Adv Polym Sci 1984;60:1.
[63] Jourdan C, Cavaille JY, Perez J. J Polym Sci, Part B: Polym Phys 1989; 27:2361.
[64] Van Dommelen J, Parks DM, Boyce MC, Brekelmans W, Baaijens F. J Mech Phys Solids 2003;51:519.
[65] Duckett RA. In: Ward IM, editor. Structure and properties of oriented polymers. London: Applied Science Publisher; 1975 [chapter11].
[66] Lorenzo V, Pereña JM. Curr Trends Polym Sci 1999;4:65.